

Fig. 1. FT-IR spectra for lipoic acid, chitosan, mPEG-NHS and LACPEG (A).  $^1\text{H}$  NMR spectra for chitosan in  $\text{D}_2\text{O}$ , lipoic acid in  $\text{CDCl}_3$  and LACPEG in  $\text{CDCl}_3$  (B). The spectrum for LACPEG contains peaks from the separate components, with an additional peak representing amide bond formation. Grey line represents water content present in chitosan. These spectra confirm LACPEG synthesis. Abbreviations:  $\text{D}_2\text{O}$ : deuterium oxide and  $\text{CDCl}_3$ : deuterated chloroform.

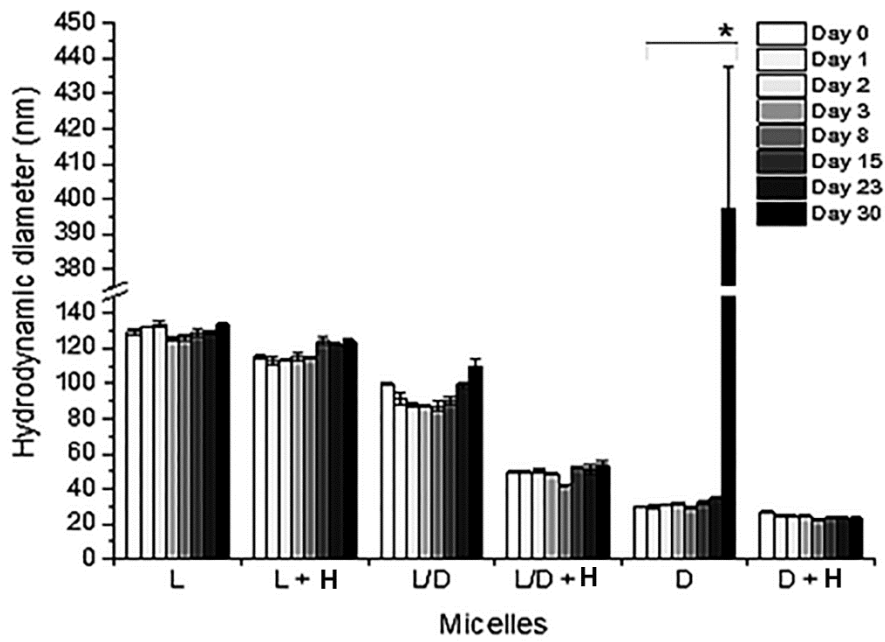


Fig. 2. Hydrodynamic diameters of empty and drug-loaded micelles. Micelles maintained their size throughout the 30 day period, with the exception to DSPE-PEG micelles, which showed aggregation at day 30 ( $*p < 0.01$ ). The use of LACPEG or entrapment of the hydrophobic drug improved micelle stability. Abbreviations: H: hydrophobic drug, L: LACPEG, L/D: LACPEG/DSPE-PEG and D: DSPE-PEG. Results are expressed as mean  $\pm$  SD (n=3).

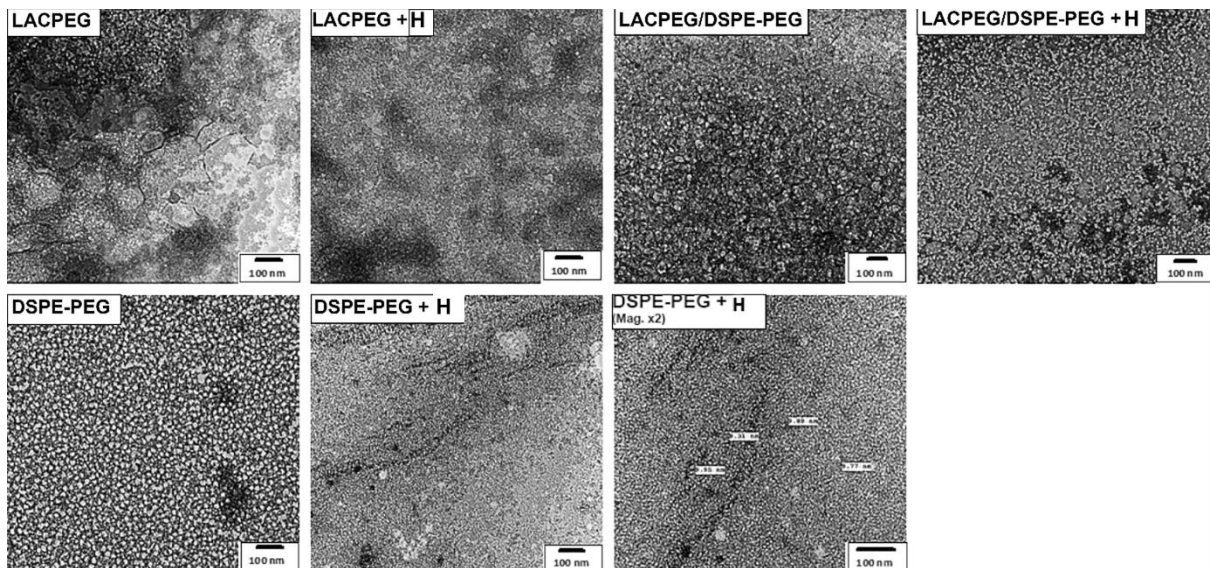


Fig. 3. Transmission electron micrographs of micelles. Abbreviation: H: hydrophobic drug.

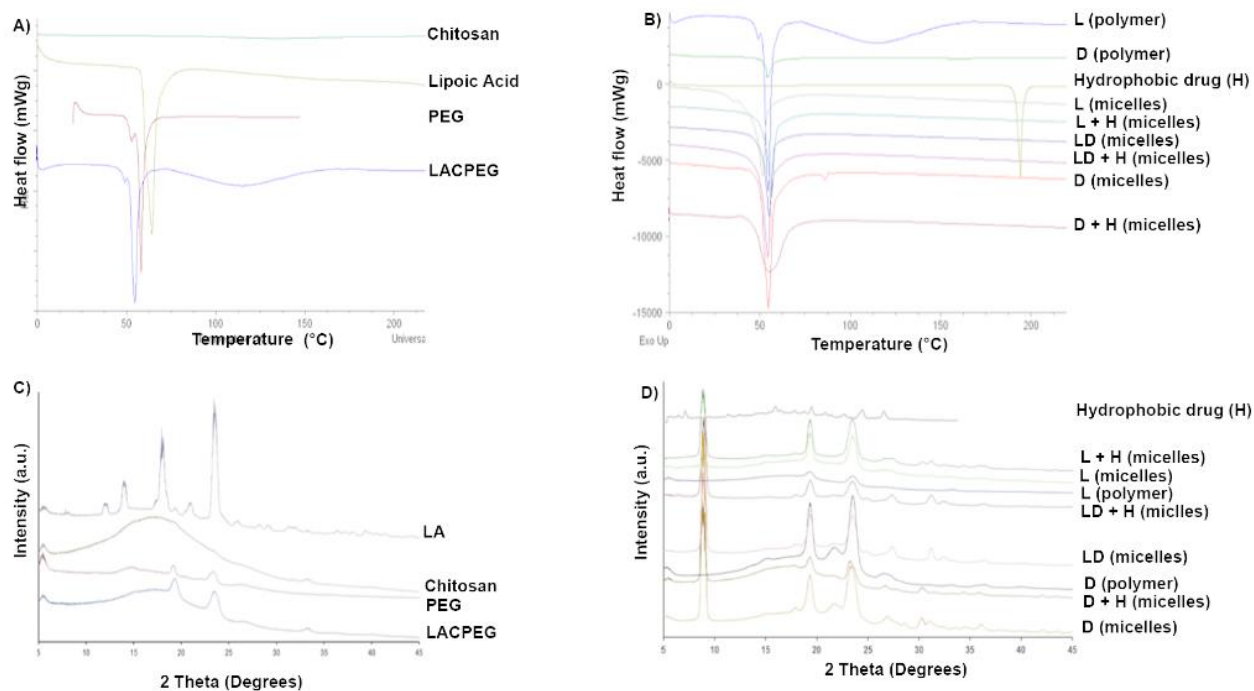


Fig. 4. DSC thermograms for chitosan, lipoic acid, poly(ethylene glycol) and LACPEG (A). LACPEG had similar thermal properties to its native constituents (chitosan, PEG and lipoic acid), showing a bifurcated peak and a broad water loss peak. DSC thermograms for empty and hydrophobic drug-loaded LACPEG and DSPEPEG micelles and their native constituents (B). The thermogram for the hydrophobic drug had a single endothermic peak at 194.1°C. Empty and drug-loaded micelles had melting temperatures in the range of 47.1°C - 56.4°C. Drug entrapment resulted in the formation of micelles with a more thermally-stable polymorphic form. XRPD diffractograms for chitosan, lipoic acid, PEG and LACPEG (C). PEG and lipoic acid showed crystalline properties. Chitosan and LACPEG had semi-crystalline properties. XRPD diffractograms for empty and drug-loaded micelles and their native constituents (D). Micelles showed semi-crystalline properties. Abbreviations: PEG: poly(ethylene glycol); LACPEG: lipoic acid-chitosan-poly(ethylene glycol); L: LACPEG, D: DSPE-PEG and H: hydrophobic drug.

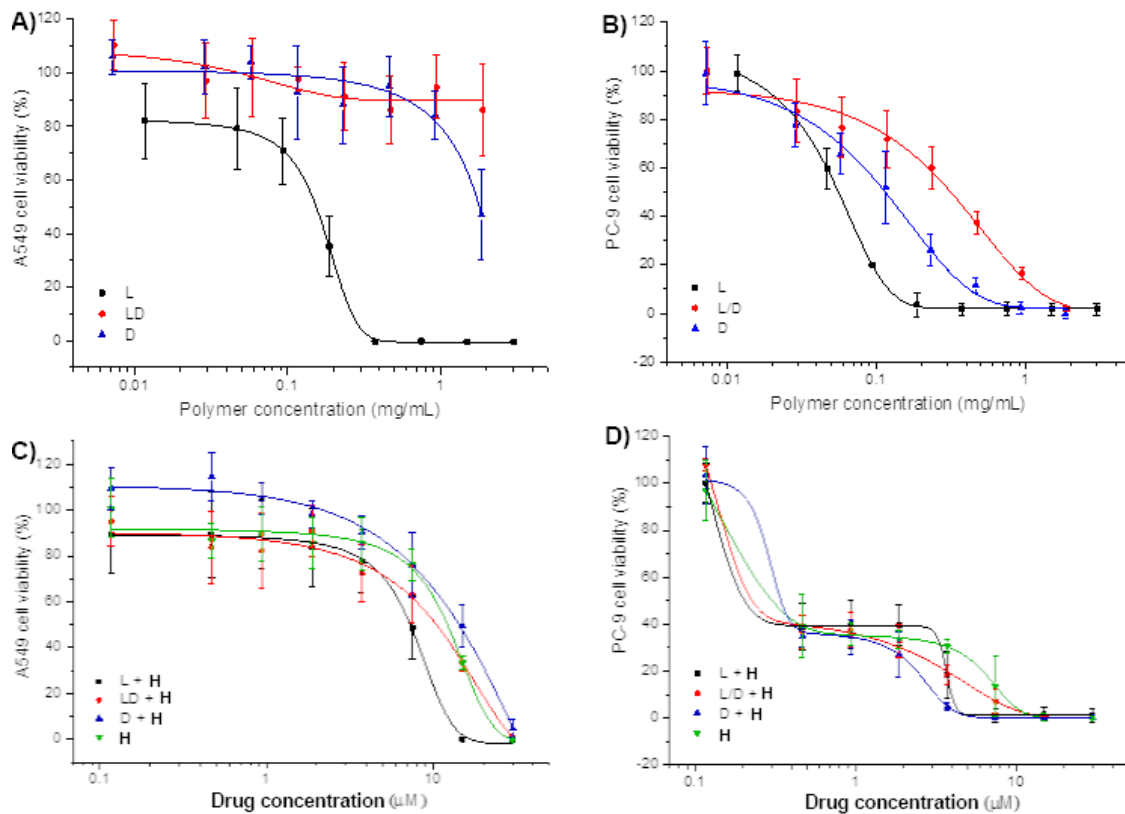


Fig. 5. Viability for A549 and PC-9 cells exposed to empty micelles (A and B), drug alone and drug-loaded micelles (C and D) at concentrations indicated for 72 h. The concentration of micelles in the drug-loaded micelles (Fig. 5 C and D) was equivalent to the range used in the empty micelles (Fig. 5 A and B). Empty micelles showed a reduction in the viability of both cell lines in the order of LACPEG > DSPE-PEG > LACPEG/DSPE-PEG. Greater cell death was obtained with drug-loaded LACPEG micelles compared to drug-loaded DSPE-PEG and LACPEG/DSPE-PEG micelles, as empty LACPEG micelles showed the greatest toxicity and this contributed to the toxicity observed with the drug-loaded micelles. All of the tested formulations caused greater cell death in PC-9 cells compared to A549 cells. Abbreviations: L: lipioic acid-chitosan-poly(ethylene glycol); D: DSPE-PEG and H: hydrophobic drug. Results are expressed as mean  $\pm$  SD (n=9).

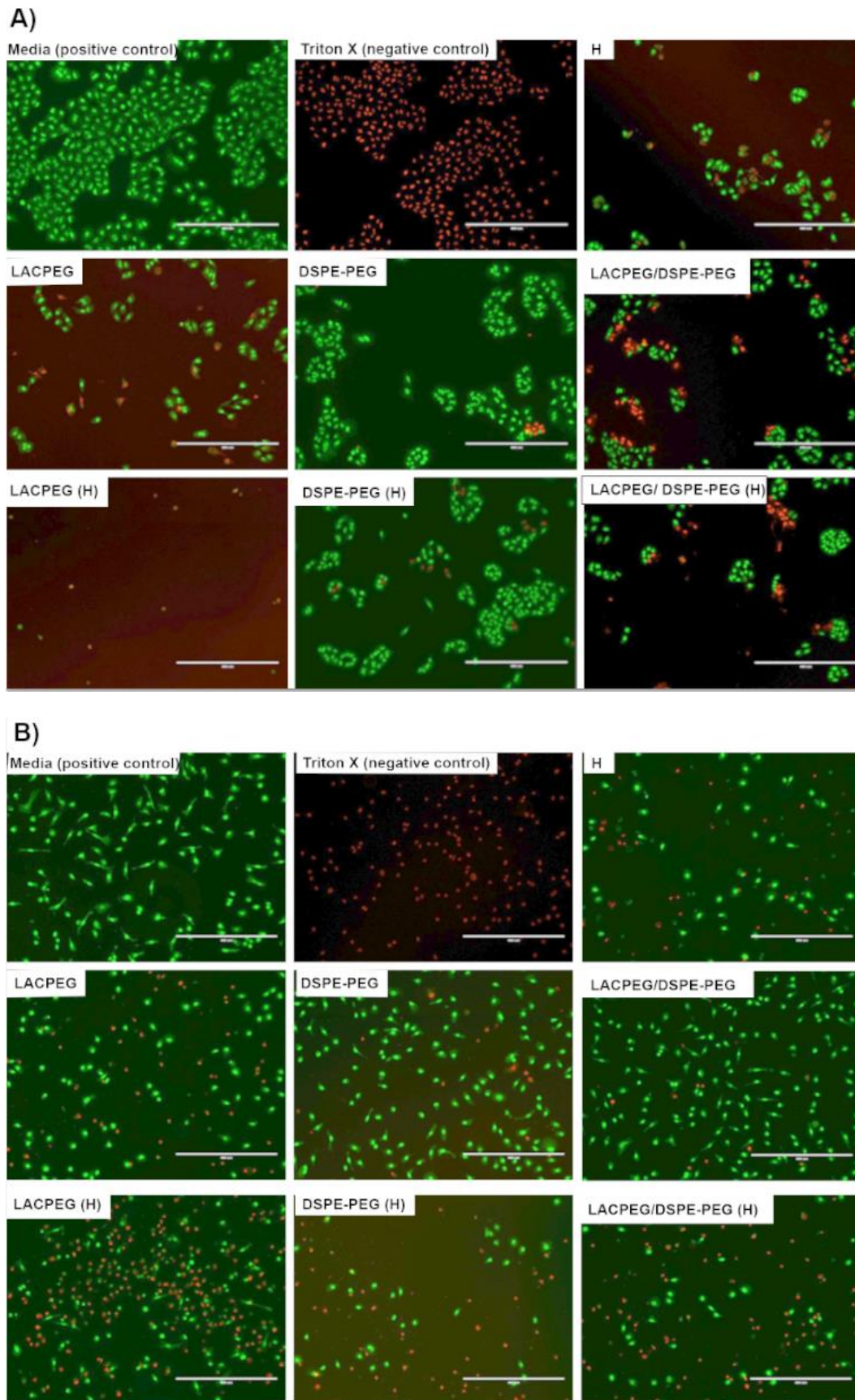


Fig. 6. Live-dead fluorescence images of A549 (A) and PC-9 (B) cells, exposed to drug solution, empty and drug-loaded micelles for 72 h. Controls used in this study were media-treated (positive) and Triton-X-treated (negative) cells. Abbreviation: H: hydrophobic drug. The images depict a greater proportion of dead (stained red with propidium iodide)

compared to living (stained green with SYTO 9) cells for the drug-loaded micelles compared to the empty micelles and drug solution.

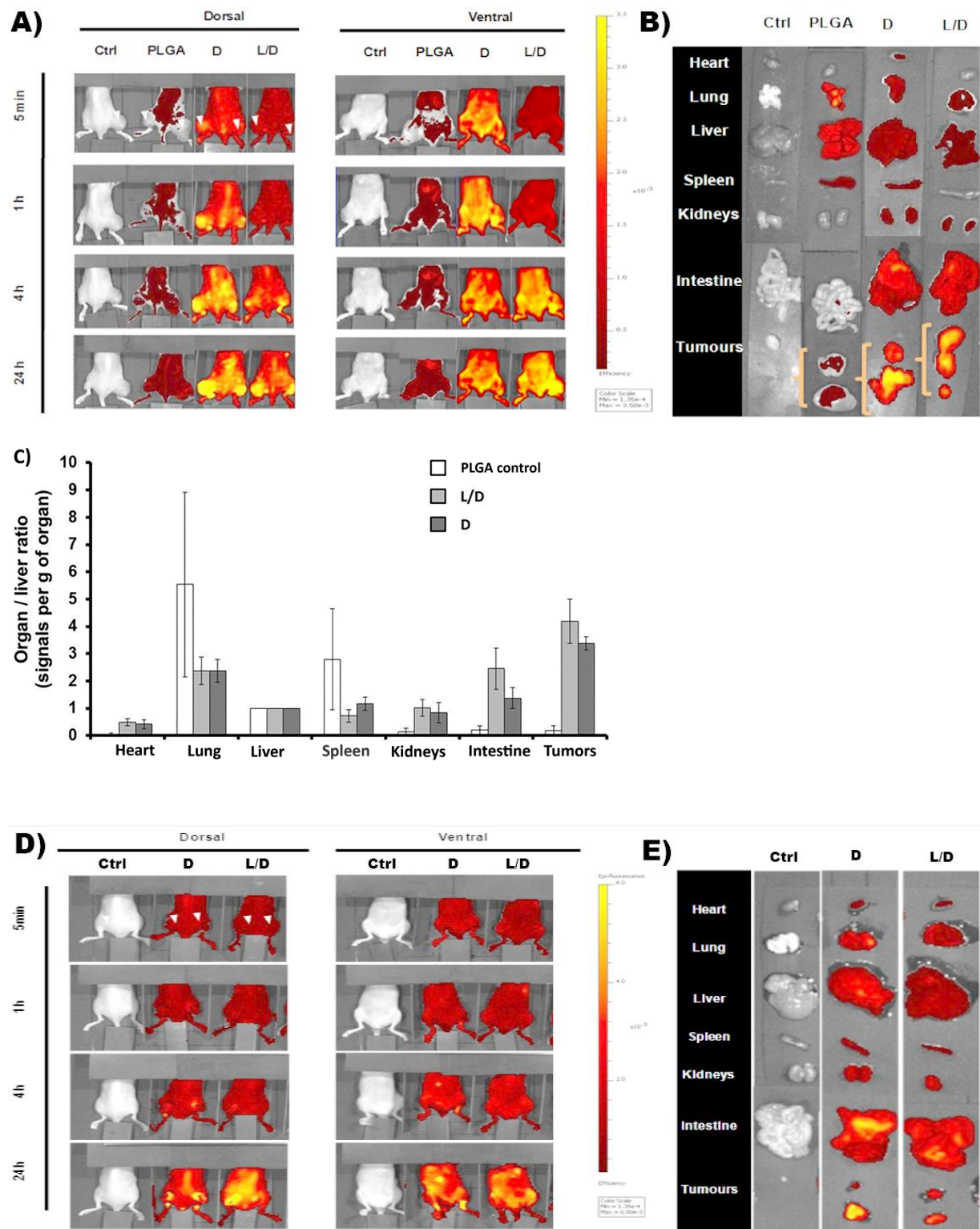


Fig. 7. *In vivo* bioluminescence imaging of DiI-incorporated micelles in CT-26 tumor-bearing BALB/c mice (A). Mice were intravenously injected (500 mg/kg dose, DiI dose administered varied with entrapment efficiency) into the tail vein and

whole body dorsal and ventral images taken over a 24 hour period (white arrows signify tumors). Control mice were injected with PBS solution. Prolonged whole body circulation and tumor accumulation was obtained for the micelles compared to the PLGA microparticles (negative control), which showed higher signals in the liver and spleen. *Ex vivo* bioluminescence studies for DiI-incorporated micelles in CT-26 tumor-bearing BALB/c mice images (B) and quantification of fluorescence signals for excised organs and tumors at 24 h, normalised to the liver (C), confirmed *in vivo* results. *In vivo* (D) and *Ex vivo* (E) bioluminescence imaging of DiI-incorporated micelles in LLC tumor-bearing C57/BL6 mice. All images were obtained by IVIS Lumina® III at exposure time: 3 s; binning factor: 4; f number 2, field of view: E-25 cm;  $\lambda_{ex}$ : 480, 500, 520, 540 and 560 nm;  $\lambda_{em}$ : 620 nm. Results are expressed as mean  $\pm$  SD (n=3) for A, B and C and n=1 for D and E. Abbreviations: D: DSPE-PEG and L/D: LACPEG/DSPE-PEG.

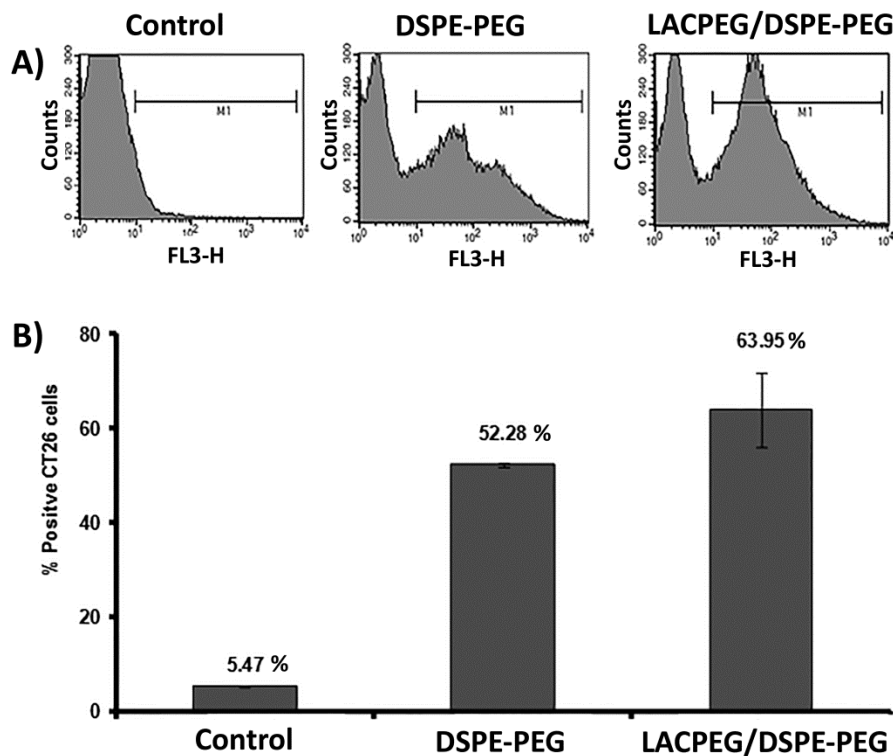


Fig. 8. Flow cytometric analysis of tumor uptake for DiI-incorporated micelles in CT26 tumor-bearing BALB/c mice. Histograms (A) and percentage (B) of DiI-positive tumor cells for each formulation are depicted. An FL-4 laser was used to analyse the tumor cells 24 h after micelle administration. Control mice were injected with PBS solution. DSPE-PEG and LACPEG/DSPE-PEG micelles showed a higher percentage of DiI-positive tumor cells compared to the control ( $p < 0.05$ ) but not from each other ( $p = 0.05$ ). Results are expressed as mean  $\pm$  SD (n=3).